Analysis of soot emissions through the development of phenomenological soot model using gasoline-ethanol blend for gasoline compression ignition combustion: A CFD Simulation Study

Abstract:

In the current study, computational fluid dynamics (CFD) simulation was performed of a single-cylinder gasoline compression ignition (GCI) engine of gasoline-ethanol blend ratios of E10 and E50. The engine CFD model was validated against experimental data collected at -25 CAD SOI1 timing. The model was validated for RD5-87 which showed similar characteristics of E10 with 87% iso-octane and 13% n-heptane by mass fraction. The trend of soot emissions increment was observed with a change in SOI1 timings which showed SOI -31 > SOI -25 > SOI -19 CAD aTDC. The effect of SOI1 timing and fuel composition were studied which showed E50 has lower soot emissions compared to E10 which was due to higher oxygen content on ethanol causing the soot to get oxidized. Soot oxidation was found to be higher for -19 CAD due to higher OH radical formation within the cylinder. Soot number density was also measured and found to be higher for the E10 case as compared to E50 for SOI timing of -31 CAD.

Introduction:

The automotive industry is currently pushing toward zero-emission vehicles. Biofuels are also gaining increased attention as alternatives to petroleum-based motor vehicle fuels, such as the Renewable Fuel Standard in the 2007 Energy Independence and Security Act [1]. The demand for improving fuel economy, reducing particulate matter emissions, and reducing greenhouse gases has driven the need for high-efficiency and cleaner IC engines. Gasoline compression ignition (GCI), which falls under the category of low-temperature combustion (LTC), aids in achieving higher efficiencies and lower emissions than conventional diesel CI engines.

In GCI, the gasoline fuel is direct injected into the combustion chamber and compression ignited. The engine performance depends on several factors like fuel injection parameters, intake charge composition, compression ratio, piston bowl geometry, and fuel reactivity [2] [3]. Each parameter has a significant effect on composition and thermal stratification in the cylinder, impacting auto-ignition and emissions characteristics. A study was done by Pal et al. [4] on several parameters that affects the combustion characteristics of a medium-load GCI engine. From the given study it was found that the start of injection timing was the main parameter affecting autoignition timing and temperature and pressure at IVC conditions. Similarly, the injection pressure was also found to be an important factor affecting the combstion duration. Beside that, the temperature at IVC was found to be the factor for soot emissions. In an experiment and numerical study done by Ra et al. [5] regarding the effect of SOI timing (-2º aTDC to -45° aTDC) on autoignition, CO, uHC, soot emissions, and oxides of nitrogen (NOx), using a multiple injection strategy for a heavy-duty engine. From this study, the advancement in injection timing resulted in maximum pressure rise rate and advanced ignition timings whereas advancing SOI timings beyond -40º aTDC showed no significant effect on ignition timing. Due to a lower gas temperature in the expansion stroke, there was a decrement in soot and NOx emissions. A CFD study done by Kodavasal et al. [3] of a light-duty GCI engine under low load conditions to characterize the impact of SOI timing on combustion characteristics. The charge reactivity was found to be reversed beyond a critical SOI timing (-30° aTDC); charge reactivity increased until the SOI timing, while it decreased with further advancement of injection

timing. This reduction was related to the fuel injected to split between the piston bowl and the squish region as the SOI timing was advanced beyond the critical SOI timing.

There has been studies to identify alternative fuels which when blended with gasoline achieves better combustion stability and lower emissions under a wide range of operating conditions. Zhang et al. [6] performed a computational study regarding significance of Octane Sensitivity (S), Research Octane Number (RON) and various physical properties on soot emissions and combustion phasing. A lower fuel reactivity allowed more mixing time before ignition, resulting in leaner local equivalence ratios and lower soot emissions. Further, to improve the combustion stability of GCI engines, various studies considered blending gasoline with ethanol [7]. In addition to reactivity, the oxygen content in the fuel aids in suppressing soot emissions. In a study done by Woo et al. [7] regarding the effect of intake-air temperature when ethanol is used as a sole fuel under CI engine conditions, ethanol showed much higher fuel conversion efficiency, despite having 36% lower calorific value than diesel. Similarly, Wu et al. [8] found reduction in soot particles of 17-44% upon the addition of 5-10% of ethanol to premixed ethylene flames, but McEnally and Pfefferle [9] and McNexby et al. [10] observed soot levels to increase when adding 10% ethanol to non-premixed ethylene flames. In the case of E10 or E20, this increase is offset by the dilution of gasoline aromatic content from blending of ethanol and, hence, low levels of ethanol would have little effect on soot levels [11]. So, gasoline-ethanol blends are a potential alternative fuel for GCI engines. They have a high oxygen content, high resistance to auto-ignition, and high evaporative cooling, all of which could further improve the already high efficiency, energy sustainability, and low emissions of GCI which are NOx and soot [12].

Different simplified soot models have been proposed. The first is for engine simulation which is a two-step model proposed by Hiroyasu et al. [14] in 1983. Due to its ease of implementation into CFD codes, this model and its modifications have acquired wide popularity in the community engaged in multi-dimensional engine simulations [15] [16]. Nevertheless, Hiroyasu et al.'s model is an empirical description, in which the particle growth and dynamics of soot are not taken into account. Soot models proposed by Kennedy et al. [17] and Moss et al. [18] linked explicitly to the fuel concentration, which in many cases is not in agreement with experimental results. They have also demonstrated that their approach can give new modified results but, neither of them received much attention due to not having larger applications. Leung and Lindstedt [19] argued that the intermediate species contributing to the soot particle formation should be connected to at least the pyrolysis kinetics of fuel. So, they assumed acetylene to be the intermediate species and developed a new soot model combined with the gas-phase kinetics of fuel pyrolysis for counterflow, and propane flames as well as co-flow, methane flames [20]. From these, good agreement was observed in soot volume fraction, particle growth, and number density. Leung and Lindstedt's model has since formed the basic model for all other soot models [21]. In the present work, I will be discussing the development of an improved soot model that has essentially the same structure as Leung and Lindstedt’s model. Thus, the phenomenological soot model with major generic processes of soot formation was proposed, which is one of the most extensively investigated soot models in recent days.

In the current study, we will be exploring the potential of how different blend ratios of ethanol to gasoline (E10 and E50) affect soot formation using the phenomenological soot model. The engine soot models have undergone a process from very simple and phenomenological to complicated kinetic models, which can be divided into purely empirical correlations, semi-empirical correlations, and detailed soot models [22]. The following section explains the methodology used and the details of how the model predicts soot formation in GCI combustion.

Modeling Methodology:

CFD Model Computational Framework

A 3D CFD model was created using CONVERGE CFD software. Different parts such as cylinder head, liner, piston, intake and exhaust ports, valve stems, valve seats and valve faces were imported using STL format. A RNG k- ε model is used for turbulence modeling. Similarly, the atomization and breakup of fuel droplets is modeled via the Kelvin-Helmholtz and Rayleigh-Taylor (KH-RT) hybrid model. This model considers the instabilities of both Kelvin-Helmholtz and Rayleigh-Taylor due to the combination of which a realistic atomization and breakup could be predicted. Figure 1 shows the computational model developed for the single-cylinder GCI engine. A 3mm base grid was prescribed throughout the entire geometry and then the grid was refined to 0.75mm inside the combustion chamber, 0.3mm around the intake and exhaust valves in the area where the incoming or outgoing fluid flows when the valves were open, 0.18mm around the injector during the injection event and 1 mm near the piston crown to resolve near-wall conditions better using the fixed embedding method.

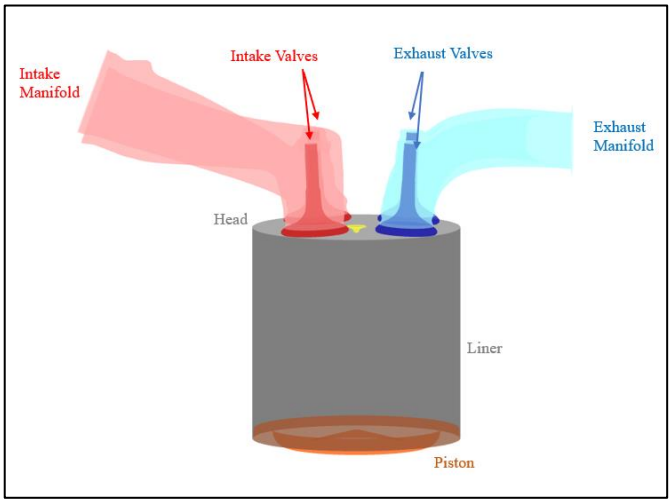

Figure 1 Computational model developed for GCI Engine

The dynamic drop drag model of Liu et al. [23] was used for the calculation of the droplet drag coefficient. This model calculates the drop drag coefficient dynamically as the flow condition changes to determine a more accurate drag coefficient. Similarly, for drop evaporation, the Frossling correlation was used which is needed to convert liquid into gaseous vapor and to determine the time rate of change of droplet size. Finally, a spray sub-model was also used to describe the interaction between the fuel spray and the engine walls. Table 1 lists the specifications of this engine.

Table 1 Specifications of single-cylinder GCI engine

Bore	82mm
Stroke	80.1mm
Connecting Rod Length	152.4mm
Geometric Compression Ratio	15.6:1
Intake Opening/ Closing	-360/-150 CAD aTDC
Exhaust Opening/ Closing	127/358 CAD aTDC
Engine speed (rpm)	1500

The specifications of the GDI injector and its specifications is provided in Table 2.

Table 2 Injector Specifications

No. of nozzle holes	8
Nozzle diameter [µm]	110
Spray included Angle [°]	150
Spray Cone Angle [°]	17
Nozzle Discharge Coefficient [-]	0.79
Experimental operating pressure [bar]	10
Injection duration	5.9 CAD
SOI	-25 CAD, 0 CAD
Injection pressure	700 bar

SAGE detailed chemistry solver was used to simulate the in-cylinder heat release developed by Seneca et al. [24]. Presently, RD5-87 gasoline containing 10% (by volume) ethanol that has an anti-knocking index of 87 was used as the baseline fuel [4]. So, PRF blend of 87% iso-octane and 13% n-heptane by mass fraction replicated the behavior of RD5-87 at these conditions [25] for E10 fuel. Similarly, the chemical properties of E50 fuel were referred and used to simulate the model. The chemical kinetics reactions and pathways were given by a 48-species, 152-reactions skeletal PRF mechanism for gasoline developed by Liu et al. [26]. Emissions formation levels except for soot are predicted according to this mechanism. A phenomenological soot model was used for the production and oxidation of soot mass as discussed in the following section.

Phenomenological soot model

In this study, a modified phenomenological soot model was constructed based on Tao's model [15] which is one proposed by Leung and Lindstedt that will predict the soot formation in the following four global stages:

a) Soot inception/ nucleation

The first critical step in soot formation is the soot particle inception or nucleation. Leung and Lindstedt [19] postulated a single-step reaction for soot nucleation, the rate of which was set to be proportional to the acetylene concentration. Later, Lindstedt [20] improved the nucleation model by including an additional step, which links benzene directly to embryonic soot particles. The sizes of initial soot nuclei were set to be of the order of 1.0nm. In the current study, we will be following the ideas of Linstedt et al.'s work [19] [20].

b) Surface growth

It involves heterogeneous reactions that contribute to the growth of mass of soot particles. This process is often approximated either by the adsorption of acetylene model. The model proposed by Harris and Weiner [26], describes the process using an apparent, first-order rate expression which is

proportional to the partial pressure of acetylene, pC_2H_2, and the total surface area of soot particles per unit volume (m^2/m^3), A_{soot}, as

$$k_{C_2H_2} p_{C_2H_2} A_{soot}.$$

The rate coefficient decays exponentially with time, and since it is difficult to implement such rate coefficient in the analysis, Arrhenius-type rate is often employed in the modeling instead [19].

c) *Surface oxidation*

Soot oxidation is a heterogeneous process that takes place on the soot particles surface and depletes the carbon atoms accumulated. It is commonly described using formulations such as the Nagle and Strickland-Constable semi-empirical model [27] to account for oxidation of soot particles. This model is adopted in the present study.

In a study done by Fenimore and Jones [28] it was found that in flame environments, about 10% of collisions with OH radicals are effective in the removal of a carbon atom.

d) *Particle coagulation*

Particle coagulation causes the soot particles number decrease. Here, we assume a monodisperse size distribution of the particles and then describe the coagulation by the Smoluchowski equation [29] as

$$\omega_{CO} = \frac{5}{6} k_{CO} (f_v)^{1/6} (f_n)^{11/6} ,$$

where, f_v and f_n denote the volume fraction (particle-m^3/m^3) and the number density (particles/m^3) of soot particles, respectively.

$$f_v = M_{soot} [C(S)] / \rho_{soot} ,$$

in which M_{soot} is the molar mass of soot, ρ_{soot} = 1800 kg/m^3 the density of a soot particle, and *[C(S)]* the molar concentration (particle-mol/m^3) of soot particles [15].

The improved soot model can give a good evaluation of the soot formation zones at various injection pressure conditions. The model is also capable of describing the lower soot at higher injection pressures. However, the model underpredicts the highest value of soot volume fraction [30].

Results and Discussions

Dalian phenomenological soot model was used that involves soot precursor formation, nucleation and growth, coagulation and oxidation, soot particle size distribution and emission prediction. The initialized factors for this soot model is given in Table 3 below. These factors were initialized in response to the literature study done for GCI combustion.

Table 3 Initialized factors for soot modeling

Soot inception pre-exponential factor	1e+11
Soot coagulation factor	2.0
Soot oxidation of OH collision factor	0.13
Soot surface growth factor	10500

Model Validations

The CFD model was validated for E10 fuel for four SOI timings. The experimental data was collected at -25 CAD aTDC. The experimental pressure trace is an average of 300 consecutive cycle, whereas the simulated pressure traces is taken from the result of third CFD cycle. The CFD model captures the average cylinder pressure and AGHRR reasonably well for all SOI timings. However, the gross heat release rate is slightly overpredicted by the model. This level of uncertainty is probably due to the differences between chemical kinetics mechanism and actual kinetics. It should be noted that in CFD modeling the heat release rates are usually harder to match with experimental results due to the sensitivity of heat release rate to temperature distribution and chemical kinetics mechanism.

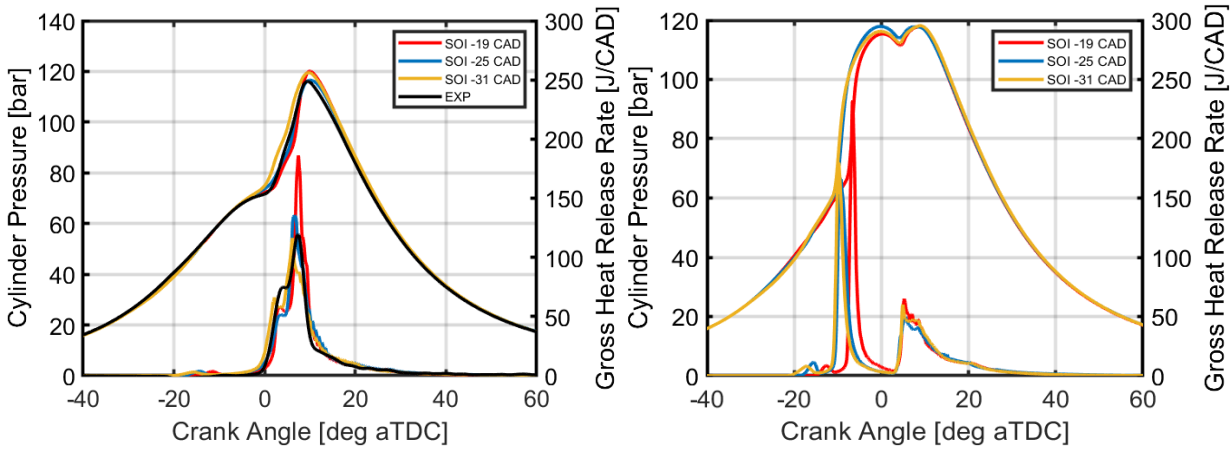

Figure 2 Model Validation for E10 (left) and E50 (right) case. CFD model was only ran for the E50 case

The time between the start of injection (SOI1) and the start of combustion is referred as ignition delay time. The ignition delay time for different SOI timings were calculated and were -19/-25/-31 CAD aTDC were 21.9/27.3/40.8 respectively. The ignition delay time was found to increase with SOI timing. This is since the in-cylinder region is cooled at initial conditions and injecting more fuel will lead to increase in the ignition delay time.

Table 4 Combustion Phasing for different SOI1 conditions for E10 fuel

SOI1 [CAD aTDC]	**-19**	**-25**	**-31**
CA0	-17	-21.5	-26.8
CA10	1.2	1.3	3.8
CA50	7.6	7.4	8.7
CA90	19.1	18.4	19.2

The ignition delay time was found to decrease with advancement in SOI1 but the combustion duration was found to decrease. The combustion duration decreases by about 1.7 CAD when SOI is advanced from -25 CAD to -31 CAD. This reduction is due to greater thermal and mixture stratification enabling autoignition to happen in a more step-by-step manner.

Table 5 Ignition Delay and Combustion Duration for E10 fuel

SOI1 [CAD aTDC]	IDT [CAD]	Combustion Duration [CAD]
-19	21.9	17.9
-25	27.3	17.1
-31	40.8	15.4

Figure 3 shows the plot of the ratio of fuel film mass on the piston to the total fuel mass injected for all SOI conditions. The ratio was increased with advancement in SOI1 for all the cases. Here, the evaporation time for the fuel film was significantly higher and is not readily available for combustion.

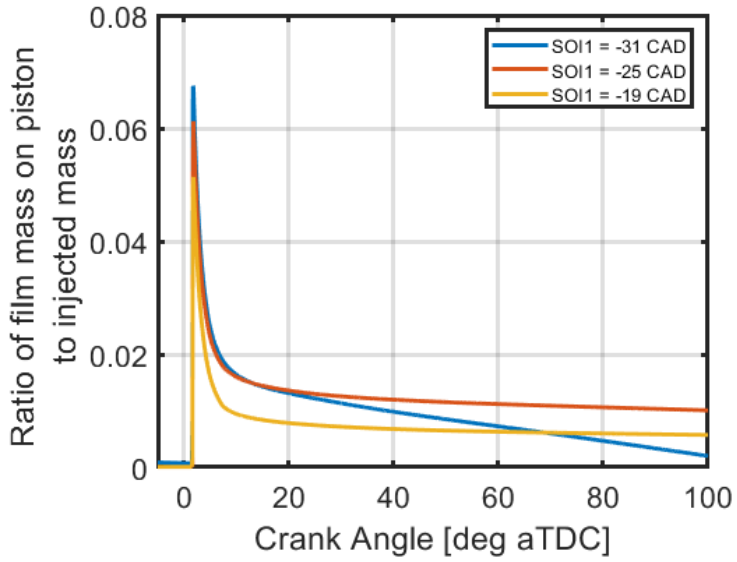

Figure 3 Ratio of fuel mass on piston to the total injected mass

The total soot mass was found to be maximum for -31 SOI1 injection timing. The soot mass found to decrease in the order of SOI -31 > SOI -25 > SOI -19. Figure 4 presents the soot emissions from E10 fuel for all SOI conditions. As we know, soot is formed in rich regions, in a temperature range of about 2000K which is due to the deposition of fuel films near wall regions. The higher temperature within the in-cylinder conditions causes fuel films to evaporate and produces more soot. In the current study, there was a significant amount of fuel film formed on the piston walls due to the impingement. It was also seen that the film mass increases with advancement in SOI1. Figure 5 shows the cut-plane visualizations for E10 and E50 fuel that shows soot mass impinging on the piston bowl (E10 > E50)

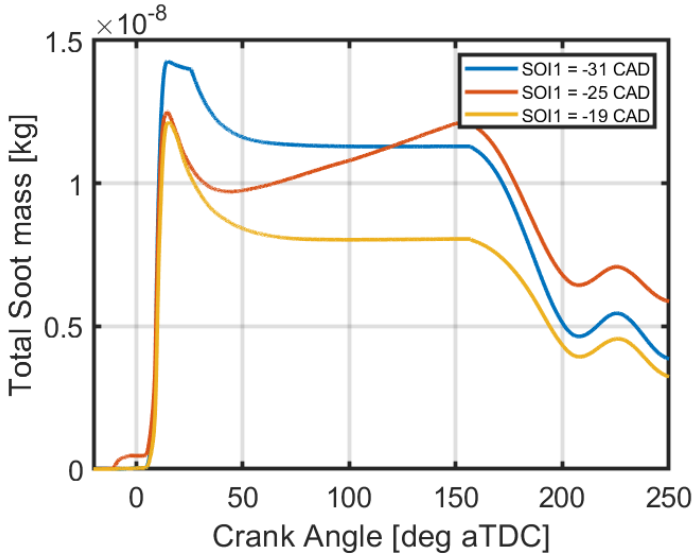

Figure 4 Total Soot mass formed for E10 fuel.

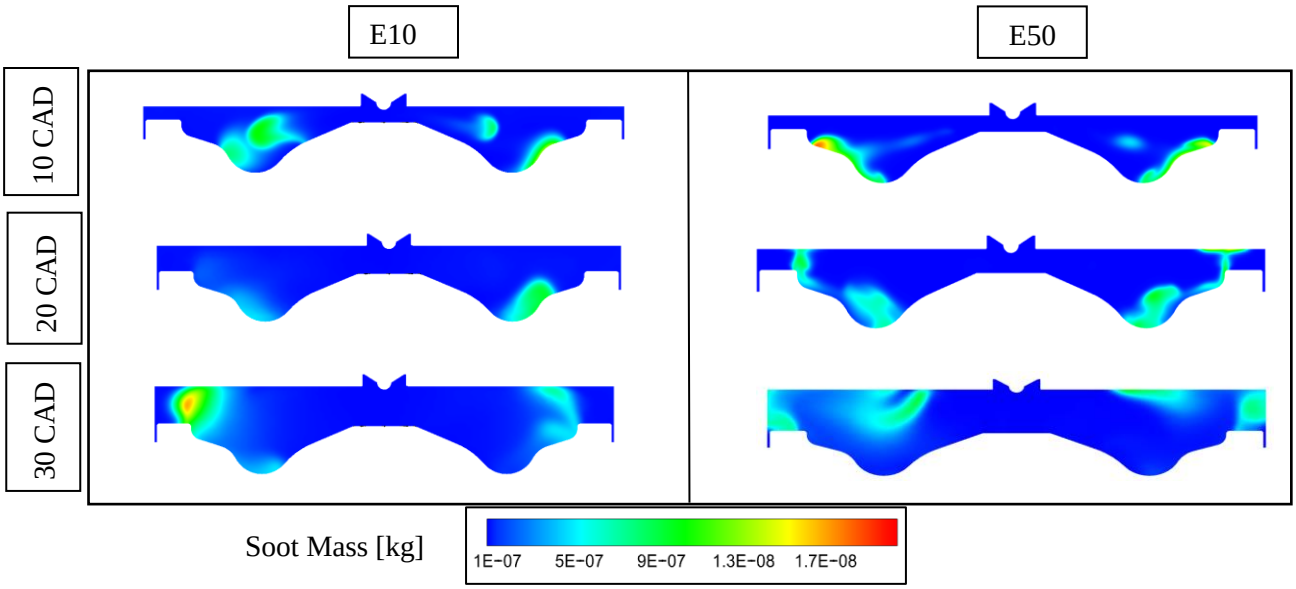

Figure 5 Cut-plane visualizations for total soot mass in (kg) for E10 (left) and E50 (right) for different crank angles 10, 20 and 30 CAD aTDC.

Like the case of E10, the total soot mass for E50 was found to be maximum for -31 SOI1 timing. The total soot mass is in the order of SOI -31 > SOI -25 > SOI -19 CAD. Figure 6 presents the soot emissions from E50 fuel for all SOI conditions. The total soot mass was comparatively low which is due to the higher oxygen content which promotes more complete combustion, resulting in fewer partially burned soot particles during the combustion process as compared to E10. The amount of peak soot mass was reduced by amount of 0.4µg as compared to both the cases.

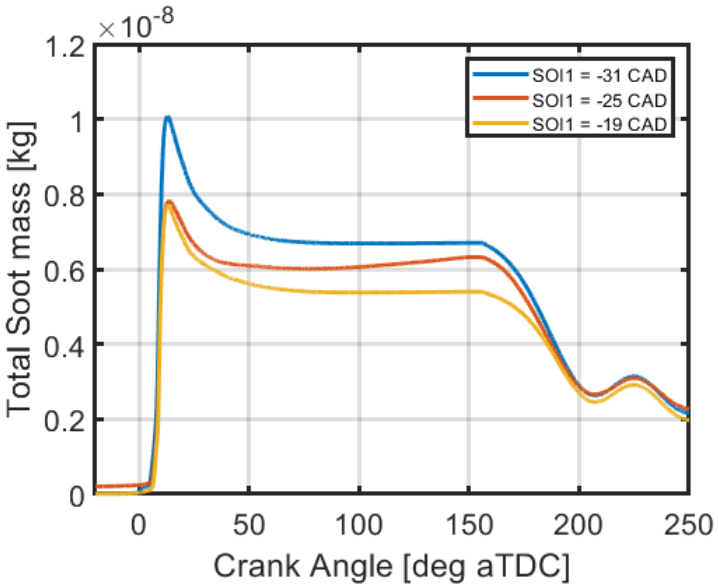

Figure 6 Total Soot mass formed for E50 fuel.

As SOI timing is advanced, it allows more time for mixing, and produces higher amount of soot for -31 CAD. This is due to the accumulation of fuel film on the walls of cylinder because of lower temperature inside the cylinder. Due to such lower temperature inside cylinder, the evaporation of liquid fuel is less that ultimately causes higher fuel film formation on the walls. Further, it is noticed that for SOI1 timing of -31 CAD, more fuel mass was near the piston bowl as compared to -25 CAD. Also, the soot oxidation process was higher due to the more amount of OH radical formed inside the cylinder. The higher amount of OH radical was formed in the cylinder at -19 CAD aTDC that causes more amount of soot to get oxidized within the cylinder causing lower amount of soot emissions.

The soot number density is also an important parameter that represents the concentration or quantity of soot particles in a unit volume within the combustion environment. Figure 7 shows the soot number density for E10 and E50 fuel. From the plots of soot number density at different SOI timings, it was found that injection timing significantly influences the formation of soot particles during the combustion process. Injecting fuel earlier in the cycle tends to increase the concentration of soot while delaying the injection timing reduces the concentration. The highest concentration of soot particles was observed at SOI timing of -31 CAD whereas the lowest was observed at SOI timing of -19 CAD.

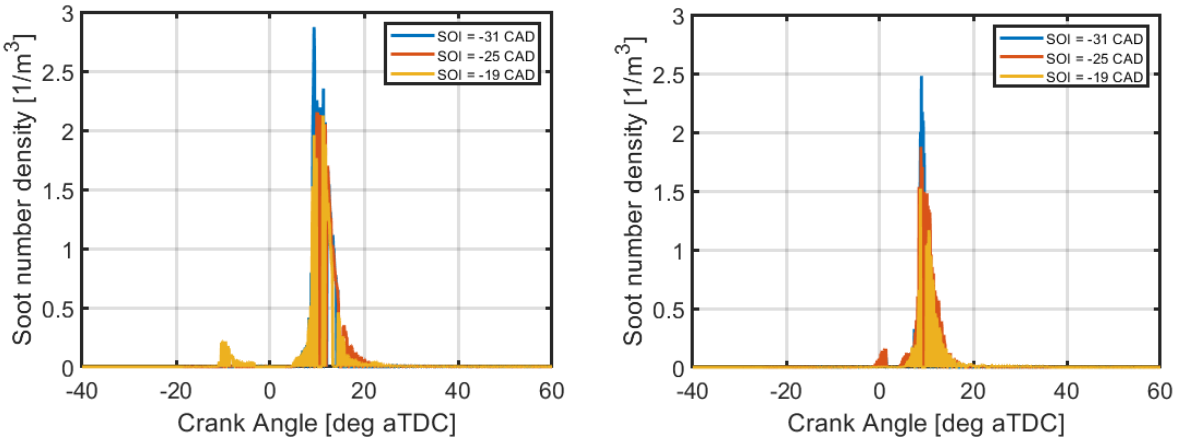

Figure 7 Soot number density for E10 (left) and E50 (right) fuel.

A higher fuel film was accumulated due to restriction in evaporation process due to cooler conditions. E10 was found to have a significant impact on combustion duration due to the higher fuel film. The heat of vaporization and viscosity of E50 is greater than E20 but both has almost similar densities. So due to higher heat of vaporization more fuel mass impinges and due to lower in cylinder temperature respective fuel film is formed with respect to E10 and E50. Further, due to the higher heat of vaporization and viscosity E50 fuel was found to have higher fuel films than E10.

The soot emissions follow the trend E10 > E50 at given SOI conditions. The soot emissions follow the trend E10 > E50 at given SOI conditions. E50 was found to produces lower soot than E10, however the fuel film accumulated for E50 is slightly higher than E10 at CA50 which is proven by the literature regarding E45 and E20. The study had showed that the physical properties of E45 and E20 play an important role in reduction of soot emissions due to the slower evaporation of fuel film and higher film mass accumulation near the piston bowl.

Conclusions

This study shows the effect of start of injection timing, and fuel composition on the soot emissions for gasoline ethanol blend ratios of E10 and E50 under ten bar conditions. The CFD model was first validated with the experimental data collected under light duty GCI engine under same operating conditions at -25 SOI1 timing. The soot emissions was found to be maximum for -31 CAD SOI1 conditions and followed the trend SOI -31 > SOI -25 > SOI -19 CAD. The amount of soot mass was found to be lower for E50 comparatively. It was identified that the due to higher ethanol content renders to produce less soot for E50 case. For the SOI timing of -31 CAD aTDC, higher amount of soot was seen which was due to higher film mass accumulation on the piston walls as compared to -25 CAD and -19 CAD. In summary, the effects of fuel composition and start of injection timing (by varying start of injection (SOI1) timing) was studied on combustion duration and soot emissions for gasoline ethanol blend of E10 and E50.

References

[1] EPA, "Transportation, Air Pollution, and Climate Change," US Environmental Protection Agency, 2007.

[2] J. K. S. C. S. S. N. S. a. J. D. Christopher Kolodziej, "Achieving Stable Engine Operation of

Gasoline Compression Ignition using 87 AKI Gasoline Down to Idle," *SAE Technical Paper,* 2015.

[3] C. P. K. S. A. C. S. S. Janardhan Kodavasal, "Computational Fluid Dynamics Simulation of Gasoline Compression Ignition," *Journal of Energy Resources Technology,* vol. 137, no. 3, 2015.

[4] P. P. J. P. G. C. P. K. H. J. S. G. K. M. M. Krishna C. Kalvakala, "Numerical analysis of soot emissions from gasoline-ethanol and gasoline-butanol blends under gasoline compression ignition conditions," *Fuel,* vol. 319, 2022.

[5] P. L. R. K. D. E. F. R. D. R. R. D. Youngchul Ra, "Gasoline DICI Engine Operation in the LTC Regime Using Triple- Pulse Injection," *SAE International Journal of Engines,* vol. 5, no. 3, pp. 1109-1132, 2012.

[6] A. V. Y. P. M. T. D. C. Yu Zhang, "A Computational Investigation of Fuel Chemical and Physical Properties Effects on Gasoline Compression Ignition in a Heavy-Duty Diesel Engine," *Journal of Solar Energy Engineering,* vol. 140, no. 10, 2018.

[7] S. K. E. R. H. Changhwan Woo, "Effect of intake air temperature and common-rail pressure on ethanol combustion in a single-cylinder light-duty diesel engine," *Fuel,* vol. 180, pp. 9-19, 2016.

[8] K. H. S. T. L. S.-Y. L. R. S. M. L. M. C. D. L. Juntao Wu, "Reduction of PAH and soot in premixed ethylene–air flames by addition of ethanol," *Combustion and Flame,* vol. 144, no. 4, pp. 675-687, 2006.

[9] L. D. P. Charles S. McEnally, "The effects of dimethyl ether and ethanol on benzene and soot formation in ethylene non-premixed flames," *Proceedings of the Combustion Institute,* vol. 31, no. 1, pp. 603-610, 2007.

[10] A. W. M. T. N. F. C. D. R. R. S. T. A. L. Kevin L. McNesby, "Experimental and computational studies of oxidizer and fuel side addition of ethanol to opposed flow air/ethylene flames," *Combustion and Flame,* vol. 142, no. 4, pp. 413-427, 2005.

[11] M. M. Maricq, "Soot formation in ethanol/gasoline fuel blend diffusion flames," *Combustion and Flame,* vol. 159, no. 1, pp. 170-180, 2012.

[12] D. H. R. Y. S. M. B. L. Yingcong Zhou, "A predictive 0-D HCCI combustion model for ethanol, natural gas, gasoline, and primary reference fuel blends," *Fuel,* vol. 237, pp. 658-675, 2019.

[13] M. T. a. B. J. Mengqin Shen, "Effects of EGR and Intake Pressure on PPC of Conventional Diesel, Gasoline and Ethanol in a Heavy Duty Diesel Engine," *SAE Technical Paper,* 2013.

[14] T. K. M. A. Hiroyuki Hiroyasu, "Development and Use of a Spray Combustion Modeling to Predict Diesel Engine Efficiency and Pollutant Emissions: Part 1 Combustion Modeling," *Bulletin of JSME,* vol. 26, no. 214, pp. 569-575, 1983.

[15] V. I. G. a. J. C. Feng Tao, "A phenomenological model for the prediction of soot formation in diesel spray combustion," *Combustion and Flame,* pp. 270-282, 2004.

[16] Z. H. R. D. R. Song-Charng Kong, "The Development and Application of a Diesel Ignition and

Combustion Model for Multidimensional Engine Simulation," *SAE Journal of Engines,* vol. 104, no. 3, pp. 502-518, 1995.

[17] W. K. J.-C. Ian M. Kennedy, "A model for soot formation in a laminar diffusion flame," *Combustion and Flame,* vol. 81, no. 1, pp. 73-85, 1990.

[18] C. S. K. S. J.B.Moss, "Proceedings of Combustion Institute," 1988.

[19] R. L. W. J. K.M. Leung, "A simplified reaction mechanism for soot formation in nonpremixed flames," *Combustion and Flame,* vol. 87, no. 3-4, 1991.

[20] H. B. R.P. Lindstedt, "Soot Formation in Combustion: Mechanisms and Models," pp. 417-439, 1994.

[21] W. J. R. L. M. Fairweather, "Predictions of radiative transfer from a turbulent reacting jet in a cross-wind," *Combustion and Flame,* vol. 89, no. 1, pp. 45-63, 1992.

[22] W. Y. a. W. Y. Feiyang Zhao, "A progress review of practical soot modelling development in diesel engine combustion," *Journal of Traffic and Transportation Engineering,* vol. 7, no. 3, pp. 269-281, 2020.

[23] D. M. R. D. R. Alex B. Liu, "Modeling the Effects of Drop Drag and Breakup on Fuel Sprays," *SAE Journal of Engines,* vol. 102, no. 3, pp. 83-95, 1993.

[24] E. P. K. R. T. B. C. C. R. M. M. P. P.K. Senecal, "Multi-Dimensional Modeling of Direct-Injection Diesel Spray Liquid Length and Flame Lift-off Length using CFD and Parallel Detailed Chemistry," *SAE Technical Paper,* 2003.

[25] M. Y. a. R. D. R. Hu Wang, "Development of a Reduced Primary Reference Fuel Mechanism for Internal Combustion Engine Combustion Simulations," *Energy and Fuels,* 2013.

[26] D. M. a. R. D. R. Alex B. Liu, "Modeling the Effects of Drop Drag and Breakup on Fuel Sprays," *SAE Technical Paper,* 1993.

[27] A. M. W. Stephen J. Harris, "Determination of the Rate Constant for Soot Surface Growth," *Combustion Science and Technology,* vol. 32, pp. 267-275, 2007.

[28] R. S.-C. J. Nagle, "Part I," in *Proceedings of the Fifth Carbon Conference* , 1962.

[29] C. P. F. a. G. W. Jones, "Oxidation of soot by hydroxyl radicals," *Journal of Physical Chemistry,* vol. 71, no. 3, pp. 593-597, 1967.

[30] S. Graham, "Proceedings of the Combustion Institute," pp. 663-669, 1976.

[31] J. L. W. M. M. W. Y. C. S. C. L. Y. K. Z. Song Li, "Development of a phenomenological soot model integrated with a reduced TRF-PAH mechanism for diesel," *Fuel,* vol. 283, 2021.